RSC Pharmaceutics

ROYAL SOCIETY OF CHEMISTRY

PAPER

View Article Online
View Journal | View Issue



Cite this: *RSC Pharm.*, 2025, **2**, 1471

# Mitigating oxidative stress in red blood cells with quercetin-loaded liposomes: a promising strategy

Akshay Kumar,[a] Stuti Bhagat,[b,c] Kareena Moar,[a] Sanjay Singh[b,c] and Pawan Kumar Maurya *[a]

Aging is a continuous process that occurs in the body and alters many physiological and cellular functions. It leads to numerous long-term ailments such as cancer, dementia, cardiovascular diseases, *etc*. To promote healthy aging with secondary metabolites and secondary metabolites encapsulated in liposomes, this study evaluated the effects of quercetin and quercetin-loaded liposomes on the oxidative stress biomarkers (GSH and MDA) of red blood cells, as RBCs deliver oxygen to tissues and are continuously exposed to oxidative stress. Quercetin is a flavonoid and has poor solubility in an aqueous medium; hence to enhance its bioavailability, it was encapsulated in liposomes. In this study, 34 healthy individuals of both sexes took part. An *in vitro* study was performed with RBCs of different age groups, namely, young, middle, and old. *tert*-Butyl hydroperoxide (*t*-BHP) was used as a positive control, while quercetin and quercetin-loaded liposomes were used as treatment agents to check their effects on GSH and MDA levels. The study showed a significant ($p < 0.0001$) increase in GSH levels and a significant ($p < 0.0001$) decrease in MDA levels in the case of quercetin-loaded liposomes. The results of the current study indicated the antioxidant role of quercetin-loaded liposomes throughout the aging process. These findings hold significant promise in the area of biomedical research and further investigation is needed to use quercetin-loaded liposomes as a potential anti-aging agent and promote health and disease-free aging.

Received 21st April 2025,
Accepted 21st July 2025

DOI: 10.1039/d5pm00112a

rsc.li/RSCPharma



## Introduction

Aging is a complex biological process marked by the gradual deterioration of inherent physiological functions over time and it finally leads to death.[1,2] Aging is associated with various health abnormalities such as cancer, dementia, and cardiovascular diseases. The average lifespan of most species is indirectly proportional to the rate of aging.[3] Aging is also linked with a decrease in ATP synthesis, an increase in ROS generation, and a reduction in antioxidant defense.[4] Increased ROS concentrations can severely damage cells, membranes, lipids, DNA, and proteins and induce oxidative stress. Several known oxidative stress biomarkers are used to study the aging process. Glutathione and malondialdehyde are the key biomarkers of aging.[5,6] MDA is present in both conjugated and unbound forms in urine, where it is eliminated after continuous circulation in the bloodstream. In particular, it indicates lipid peroxidation, making it the most evaluated biomarker for oxidative stress.[7] An essential hydrophilic antioxidant present in erythrocytes is GSH. Reduced glutathione (GSH) is the other biomarker that is frequently evaluated. It is a tripeptide made up of three amino acids. Age and erythrocyte GSH levels are negatively correlated, and it is also linked to plasma's overall antioxidant potential.[8]

Quercetin is a most abundant flavonoid, belonging to a subclass of flavanols found in red onions and many other plants. Quercetin is widely recognised for its antioxidant, anti-inflammatory, anticancer, neuroprotective, and cardioprotective properties.[9–11] Quercetin comprises two aromatic rings (A and B) connected by an oxygen-containing heterocycle (ring C) and features hydroxyl (OH) substituents at positions 5 and 3. Due to its unique structure, quercetin is extensively employed as a beneficial dietary supplement, recommended for mitigating and preventing various diseases linked to oxidative stress.[12] Quercetin has a very low oral bioavailability (1%) in humans because of its low aqueous solubility (~1 mg $mL^{-1}$ in water, ~5.5 mg $mL^{-1}$ in simulated gastric fluid, and ~28.9 mg $mL^{-1}$ in simulated intestinal fluid) and inefficient uptake in the digestive system.[13,14] Despite having a broad range of pharmacological characteristics, quercetin's limited solubility in water and instability in physiological media limit its use in the pharmaceutical industry. This instability not only hinders its absorption through the skin but also results in poor bio-

[a]*Department of Biochemistry, Central University of Haryana, Mahendergarh, 123031, India. E-mail: pkmaurya@cuh.ac.in; Tel: +91 9560869477*
[b]*DBT-National Institute of Animal Biotechnology (NIAB), Opposite Journalist Colony, Near Gowlidoddy, Extended Q-City Road, Gachibowli, Hyderabad-500032, Telangana, India*
[c]*DBT-Regional Centre for Biotechnology (RCB), Faridabad–121001, Haryana, India*

availability and permeability. Due to its low bioavailability, quercetin does not exert its full antioxidant potential. Since nanocarriers may encapsulate both hydrophobic and hydrophilic moieties, entrapping or adsorbing quercetin into them is one method to overcome these issues.[15]

Liposomes are commonly used in nanomedicine because of their high drug-loading efficiency, stability, ease of synthesis, and high bioavailability.[16] Liposomes consisting of lecithin and cholesterol are most popularly used as safe excipients because of their capacity to enclose medicinal molecules in the lipophilic membrane or the tear-like interior of the vesicles.[17] Because of their special qualities, which include controlled release, biocompatibility, and the ability to transport both water-soluble and insoluble substances, liposomes are widely acknowledged as smart delivery systems for use in food, medicine, agriculture, and cosmetics.[18] As carriers for drug delivery, liposomes possess the qualities of being non-toxic, biocompatible, and biodegradable. Liposomes offer the following benefits: they are less toxic and can encapsulate both lipophilic and hydrophilic drugs which improves the solubility of drugs in an aqueous medium.[16,19] The sustainable release of a drug from liposomes boosts the bioavailability of the drug.[20] Liposomes are ideal candidates for administering drugs because of their stability and strong *in vitro* cytocompatibility, both when empty and when loaded with antioxidant compounds. Liposomes are composed of lipids similar to those found in cell membranes, making them highly biocompatible and less likely to cause adverse reactions. This is in contrast to some other nanomaterials that might trigger immune responses or have toxic effects.[21] Liposomes can encapsulate both hydrophilic (water-soluble) and hydrophobic (fat-soluble) drugs, offering flexibility in the types of molecules they can carry. Other nanoformulations might be better suited for one type of molecule over another.[22] Additionally, quercetin encapsulation can shield cells from oxidative stress damage.[23]

In order to optimize quercetin's antioxidant potential, regulated release, targeted distribution, and safety while simultaneously enhancing its therapeutic potential, we developed a liposomal formulation of quercetin and investigated its effects on oxidative stress biomarkers in RBCs, specifically MDA and GSH.

## Materials and methods

Egg phosphatidylcholine (PC), chloroform, quercetin, and cholesterol were procured from Sigma Aldrich. Reduced glutathione, 5,5′-dithiobis(2-nitrobenzoic acid) (DTNB), thiobarbituric acid (TBA), and EDTA were purchased from HiMedia India Private Limited. All other chemicals and reagents used in the study were of analytical grade.

### Collection and processing of samples

Blood samples were collected from 34 healthy volunteers in the Haryana region. The criteria for the selection of healthy individuals were as per previously published reports.[14] Briefly, the individuals did not have any major illness such as diabetes, cancer, or tuberculosis, and no pregnant and lactating women were included in this study. None of the individuals were smokers. Venous blood samples were drawn into EDTA vials from healthy human participants of different age groups. Human blood samples used in this study were obtained in accordance with the ethical standards of the Institutional Human Ethics Committee. The study protocols were approved by the Institutional Human Ethics Committee, Central University of Haryana (approval ref. no. CUH/2020/IHEC/04). Informed consent was obtained from all donors prior to sample collection. All samples were anonymized to ensure donor confidentiality.

### Synthesis of quercetin-loaded liposomes

Quercetin-loaded liposomes were synthesized by a thin film hydration method followed by sonication and extrusion.[24] Briefly, 10 mg of egg PC and 1 mg of cholesterol were dissolved in chloroform followed by the addition of 0.6 mg of quercetin (10 : 01 : 0.6). To prepare a lipid thin film, $N_2$ gas was passed through the above solution mixture. Furthermore, this film was rehydrated with 1 mL of 1× PBS and heated at 60 °C in a water bath for 30 minutes followed by vortexing every 3 min. Next, the rehydrated solution was sonicated for 30 min at 60 °C. Quercetin-loaded liposomes were extruded by using a mini extruder using a 100 nm polycarbonate membrane. The approach was also used to synthesize empty liposomes without quercetin.

### Characterization of quercetin-loaded liposomes

The UV-vis spectra of unbound quercetin and quercetin-loaded liposomes were obtained using a UV-vis double beam spectrophotometer (UV-Vis 2080Plus, Analytical Technologies Limited, India) in a 1 mL quartz cuvette. The liposomes' hydrodynamic size and zeta potential were determined using dynamic light scattering (DLS) (Anton Paar Particle Analyzer, Litesizer 500). The shape and size of the empty liposomes and quercetin-loaded liposomes were analyzed using a transmission electron microscope (TEM) (JEOL, FLASH JEM1400) through the application of the negative staining technique. During this process, liposomes were placed onto a copper grid (coated with carbon) and left to dry overnight. Afterward, the grid was subjected to treatment with a solution of 4 parts of Milli-Q water and 1 part of uranyl acetate for 30 seconds and washed 5 times with Milli-Q water. Infrared absorption spectra of quercetin, quercetin-loaded liposomes, and empty liposomes were recorded using attenuated total reflectance (ATR)-Fourier transform infrared spectroscopy (FTIR) (Thermo Scientific Nicolet iS50 FT-IR). For FTIR sample preparation, 200 mg of potassium bromide (KBr) was mixed with 100 μL of the liposomes dried under an IR lamp followed by FTIR analysis.

### Quercetin loading efficiency of liposomes

0.6 mg of quercetin was loaded into lipids at different concentrations to achieve maximum drug loading efficiency. Liposomes were disrupted in absolute ethanol followed by monitoring of the absorption of quercetin at 373 nm. The con-

centration of quercetin was estimated using a standard curve of free quercetin. The drug loading efficiency was measured using the below-mentioned equation:

$$\%\ \text{Encapsulation efficiency} = (\text{drug in liposomes} \div \text{total drug}) \times 100$$

### *In vitro* quercetin release study

The release of quercetin was tested in a controlled environment at 37 °C temperature using a dialysis membrane with a molecular weight cutoff of 12.4 kDa. 1 mL of purified quercetin-loaded liposomes was placed inside the dialysis membrane and mixed with 100 mL of KRB-GSH buffer (pH 7.4) as the dialysate. At specific time points (0, 0.5, 1, 2, 3, 6, 12, and 24 hours), 100 μL samples of the dialysate were collected and the amount of quercetin released was measured using a UV-vis double beam spectrophotometer (UV-Vis 2080Plus, Analytical Technologies Limited, India) at a wavelength of 373 nm. The quercetin concentration was determined by utilising the standard curve of unbound quercetin.

### ABTS radical scavenging activity of quercetin-loaded liposomes

A stock solution of $ABTS^{\bullet+}$ was prepared by dissolving 7 mM ABTS with 2.45 mM potassium persulfate in distilled water and allowed to stand for 16 hours at room temperature in the dark. The stock solution was diluted with distilled water to create a working solution with an absorbance level of ~1.0 at 730 nm. The ABTS solution was then mixed with various concentrations (25, 50, 100, 150, and 200 μg $mL^{-1}$) of quercetin, quercetin-loaded liposomes, empty liposomes, and gallic acid at a 1 : 20 ratio and incubated for 15 minutes in the dark; measurements of the absorbance were taken at 730 nm.

### *In vitro* treatment effects of quercetin and quercetin-loaded liposomes on biomarkers of red blood cells

The estimation of erythrocyte MDA levels was conducted using a known protocol, which was previously published.[25] Briefly, 1.5 mL of Krebs–Ringer phosphate (KRP) buffer having pH 7.4 was used to suspend 0.1 mL of packed erythrocytes to start the analysis. Then, one milliliter of cell lysate was mixed with the same volume of trichloroacetic acid (TCA 10%), and the mixture was centrifuged for five minutes at 3000 rpm. Subsequently, the liquid portion was combined with an equal amount of 0.67% TBA and heated to a temperature higher than 90 °C for 30 minutes. The absorbance of the samples was measured at wavelengths of 532 nm and 600 nm after they were cooled. The net optical density (OD) was obtained by subtracting the absorbance at 600 nm from the absorbance at 532 nm. The concentration of MDA in erythrocytes were determined as nmol $mL^{-1}$ PRBCs.

To quantify the amount of reduced glutathione in red blood cells, the Beutler method was utilized.[26] Briefly, 1 mL of cell lysate was mixed with 0.5 mL of precipitating solution. This solution was centrifuged at 3000 rpm for 5 minutes. 0.5 mL of the filtrate was taken and mixed with phosphate solution. DTNB was added and the absorbance was read at 412 nm using a UV-visible spectrophotometer.

*In vitro* experiments were conducted. Quercetin and quercetin-loaded liposomes (3 μg $mL^{-1}$) were introduced into the assay medium and incubated at 37 °C for one hour before the assay. Simultaneously, control experiments were performed by incubating the assay medium without the addition of quercetin or quercetin-loaded liposomes. To induce oxidative stress *in vitro*, washed PRBCs were incubated with $10^{-5}$ M *tert*-butyl hydroperoxide.

### Statistical analysis

GraphPad Prism version 5.00 for Windows was used to perform the statistical analysis. Data are represented as mean ± standard error of the mean (SEM). The paired *t*-test was employed to assess the statistically significant associations between the variables. A *p*-value equal to or less than 0.05 was deemed to indicate statistical significance.

## Results

Quercetin demonstrates two distinctive peaks between 240 and 280 nm and 340 and 440 nm (Fig. 1A, red curve).[27] Similar peaks were observed albeit with reduced intensity in the case of quercetin-loaded liposomes (Fig. 1A, black curve). This observation supports the successful encapsulation of quercetin within the liposomes. Importantly, empty liposomes (Fig. 1A, green curve) exhibit no absorbance peak in this region, confirming that the peaks between 240 and 280 nm and 340 and 440 nm are solely due to the presence of quercetin within the quercetin-loaded nanoliposomes. The FTIR data suggested the presence of C=C stretching (1564 $cm^{-1}$), C–H bending (2016 $cm^{-1}$), O–H bending (2943 $cm^{-1}$), and O–H stretching (3248 $cm^{-1}$), which corresponds to the signature peak of quercetin, suggesting the presence of quercetin (Fig. 1B, black curve). The C–H bending at 1447 $cm^{-1}$ and the C=O stretching at a wavenumber of 1754 $cm^{-1}$ correspond to the presence of lipids in empty liposomes (Fig. 1B, green curve) and quercetin-loaded liposomes (Fig. 1B, red curve). The O–H stretching at a wavenumber of 3248 $cm^{-1}$ was present in both quercetin and quercetin-loaded liposomes. Also, the dynamic light scattering (DLS) analysis revealed a hydrodynamic size of 273 ± 3 nm for empty liposomes, contrasting with the transmission electron microscopy (TEM) measurement of 90 nm (Fig. 2A and B). Similarly, for quercetin-loaded liposomes, DLS indicated a size of 480 ± 3 nm, whereas TEM suggested a size of 100 nm (Fig. 2C and D). These discrepancies may be attributed to the presence of a solvation shell and associated quercetin molecules surrounding the liposomes, leading to larger hydrodynamic and TEM sizes compared to empty liposomes. The zeta potentials of quercetin-loaded and empty liposomes were measured at −3.43 ± 0.23 and −3.46 ± 0.53, respectively, as egg phosphatidylcholine is a neutral lipid (Table 1). Furthermore, the zeta potentials of both empty and quercetin-loaded liposomes remained unchanged, suggesting the presence of quercetin inside the liposomes.

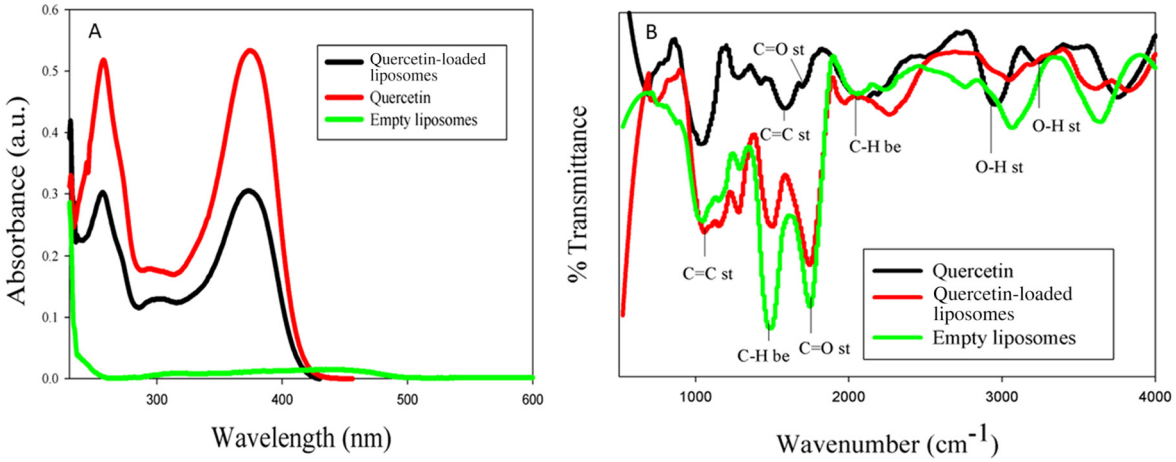


**Fig. 1** (A) UV-visible spectra of quercetin (red curve), quercetin-loaded liposomes (black curve), and empty liposomes (green curve). (B) Fourier transform infrared spectra of free quercetin (black curve), quercetin-loaded liposomes (red curve), and empty liposomes (green curve). "st" stands for stretching and "be" stands for bending.

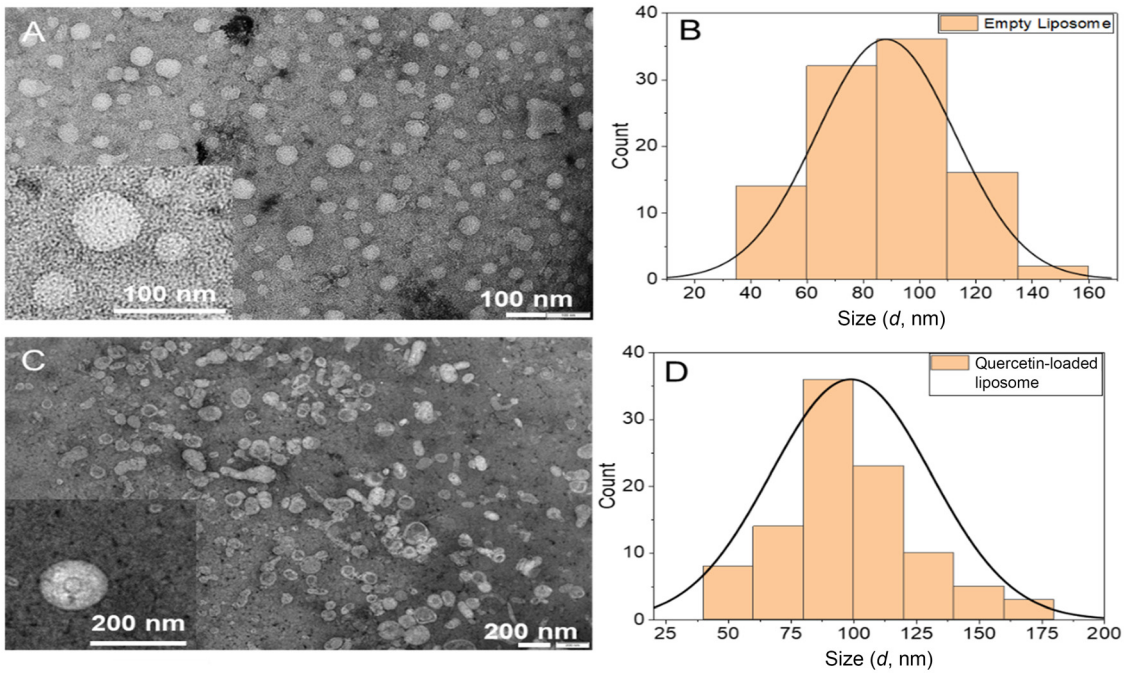


**Fig. 2** Transmission electron microscopy image of empty liposomes (A), particle size distribution of empty liposomes (B), TEM image of quercetin-loaded liposomes (C), and particle size distribution of quercetin-loaded liposomes (D). The insets show high magnification images of the respective liposomes.

**Table 1** Hydrodynamic sizes, polydispersity indexes (PDIs), and zeta potentials of empty and quercetin-loaded liposomes

| Liposomes | Hydrodynamic size (*d*, nm) | Polydispersity index (%) | Zeta potential (mV) |
|---|---|---|---|
| Empty liposomes | 273 ± 3 | 10 ± 1 | −3.46 ± 0.53 |
| Quercetin-loaded liposomes | 480 ± 3 | 18 ± 0.5 | −3.43 ± 0.23 |

The efficacy of drug encapsulation inside the liposomes was evaluated. The efficacy of drug encapsulation was determined through varying the ratio of egg phosphatidylcholine : cholesterol : quercetin at 2.5 : 0.25 : 0.600, 5 : 0.5 : 0.600, and 10 : 1 : 0.600 and found to be 37.07%, 44.11%, and 86.14%, respectively (Fig. 3). The quercetin standard curve was created using the plot of absorbance *vs.* concentration. The amount of quercetin encapsulated in the liposomes was determined using this curve. According to previously published data, the quercetin encapsulation efficiency is less than 50% in the

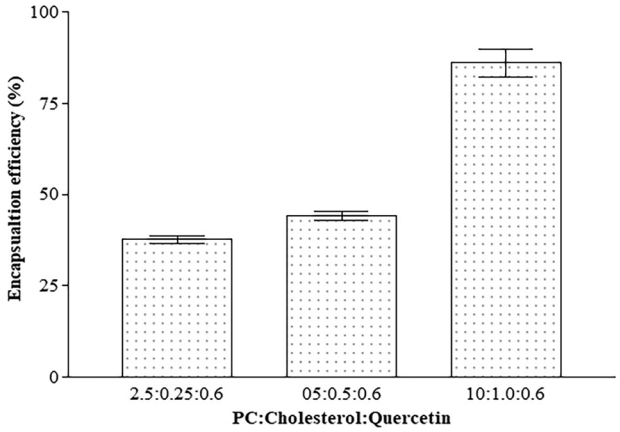


**Fig. 3** Encapsulation efficiencies (%) of various ratios of egg phosphatidylcholine : cholesterol: quercetin. Data are expressed as mean ± SEM; $n$ = 3. PC stands for egg phosphatidylcholine.

cases of phosphatidylcholine and cholesterol. In contrast, deformable liposomes containing a surfactant showed higher encapsulation efficiencies ranging from 65% to 80.41%.[28] Our results showed 86.14% encapsulation efficiency without using any surfactant. We investigated the release kinetics of quercetin from the liposomal formulation in Krebs–Ringer bicarbonate buffer in the presence of glutathione at pH 7.4 under *in situ* conditions. To mimic the conditions of red blood cells *in vitro*, we utilized KRB with GSH buffer. Drug release was assessed at different times (0, 0.5, 1, 2, 3, 6, 12, and 24 hours) as shown in Fig. 4. It was observed that ~45% (0.2323 mg $mL^{-1}$) of the drug was released from liposomes within 30 min. For the complete release (~90%, 0.4644 mg $mL^{-1}$), it took about 12 hours under *in situ* conditions. These data suggest that the developed quercetin-loaded liposomes quickly release (within 30 min) quercetin which can help reduce the dosage and improve the action of the drug.

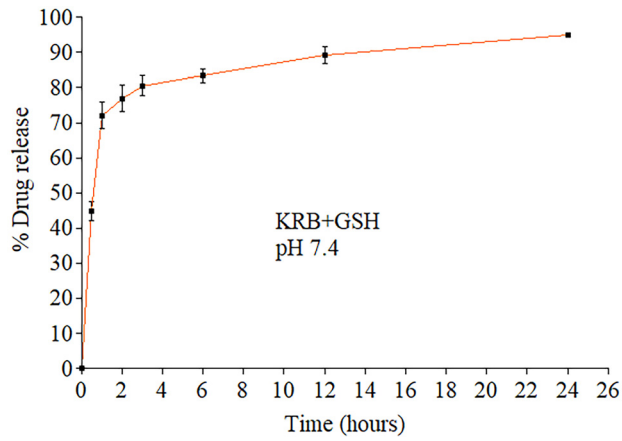


**Fig. 4** *In vitro* release of quercetin encapsulated in liposomes (KRB + GSH buffer, pH 7.4). Data are expressed as mean ± SEM; $n$ = 3. KRB + GSH buffer stands for Krebs–Ringer bicarbonate buffer with reduced glutathione.

The ABTS radical scavenging activity of all the tested compounds at various concentrations (25 to 200 μg $mL^{-1}$) is shown in Fig. 5. Quercetin-loaded liposomes and quercetin showed percent radical scavenging activity in a concentration-dependent manner, and gallic acid showed approximately similar activity at all concentrations, while empty liposomes showed a very low percent radical scavenging activity. This indicated that the ABTS radical scavenging activity comes from quercetin only. Except for empty liposomes (3.33 ± 0.30), quercetin-loaded liposomes, quercetin, and standard antioxidant gallic acid showed almost similar % scavenging activity at 200 μg $ml^{-1}$: 94.07 (±1.19), 94.30 (±0.74) and 93.75 (±0.09). At lower (25–100 μg $mL^{-1}$) concentrations quercetin-loaded liposomes have better ABTS radical scavenging activity than free quercetin. This is because the liposomal encapsulation enhances the solubility of quercetin in the medium.

*In vitro* treatment with quercetin and quercetin-loaded liposomes (3 μg $ml^{-1}$) significantly ($p < 0.0001$) decreased MDA levels in PRBCs in all age groups (young, middle, and old) compared to that in PRBCs with *t*-BHP ($10^{-5}$ M)-induced oxidative stress. *t*-BHP ($10^{-5}$ M) was used to induce a known amount of stress in PRBCs. Quercetin-loaded liposomes showed a more prominent decrease in MDA levels compared to quercetin alone in the middle and old age groups (Fig. 6).

According to our findings, the GSH level is inversely proportional to age. As aging happens the level of GSH decreases and *vice versa*. PRBCs treated *in vitro* with quercetin (3 μg $ml^{-1}$) and quercetin-loaded liposomes (3 μg $ml^{-1}$) showed significantly ($p < 0.0001$) upregulated GSH content in all age groups compared to PRBCs with *t*-BHP ($10^{-5}$ M)-induced oxidative stress (Fig. 7).

## Discussion

RBCs should have a defense mechanism against the harmful effects of free radicals because they are constantly exposed to them. In this case, we suggest that the liposomal formulation of quercetin will aid in reducing the impact of free radicals by raising GSH levels and reducing the effect of MDA levels. Although the precise process is unknown, it is thought that liposomal formulations aid in better quenching of free radicals, in comparison with free quercetin. Notable differences were observed between the size measurements obtained from DLS and TEM analysis. These discrepancies may be attributed to the presence of a solvation shell and associated quercetin molecules surrounding the liposomes, leading to larger hydrodynamic sizes than TEM sizes. To guard against the consequences of oxidative stress, the RBC membrane has a variety of defense mechanisms. During oxidative stress, the red blood cell membrane is vulnerable to lipid peroxidation, which results in the formation of MDA by the cleavage of polyunsaturated fatty acids at their double bonds.[29] The present investigation used the assumption that when cells are stimulated by t-BHP, stress occurs. The PUFA present in the RBC membrane walls undergoes peroxidation, which raises the

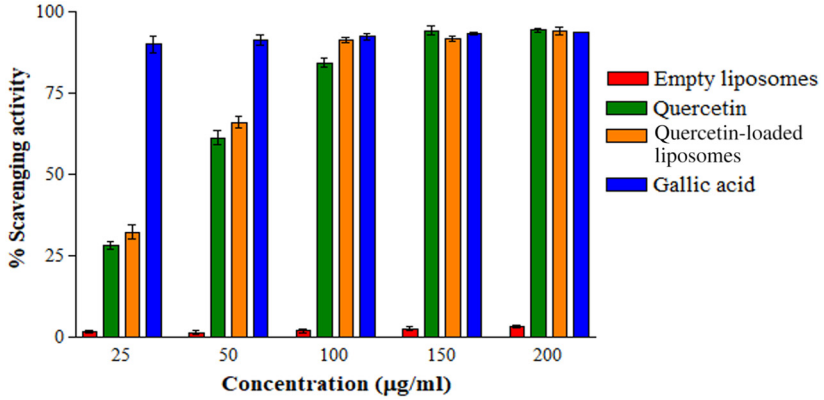


**Fig. 5** Dose dependent (25–200 μg ml$^{-1}$) antioxidant activity of empty liposomes, quercetin, quercetin-loaded liposomes, and gallic acid using ABTS (2,2′-azino-bis (3-ethylbenzothiazoline-6-sulfonic acid)) assay. Data are expressed as mean ± SEM; $n$ = 3.

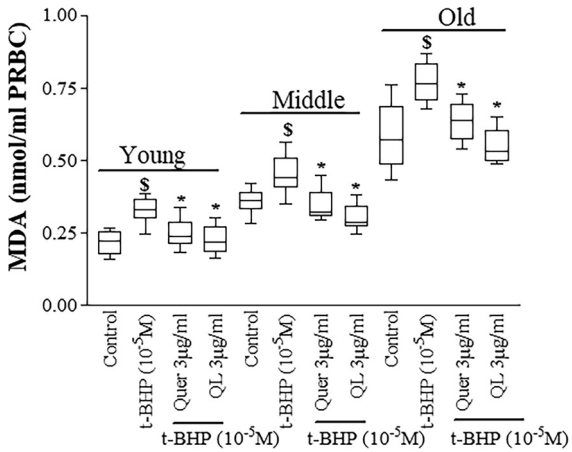


**Fig. 6** The effects of quercetin and quercetin-loaded liposome treatment (3 μg ml$^{-1}$) on MDA content under $t$-BHP-induced oxidative stress in red blood cells of different age groups, *i.e.*, young (20–35 years; $n$ = 11), middle (36–60 years; $n$ = 14), and old (>60 years; $n$ = 6). The MDA level was measured in nmol ml$^{-1}$ PRBCs. PRBCs incubated with $t$-BHP exhibited significantly increased MDA levels ($, $p < 0.0001$) compared to the control group. The Quer and QL treatment decreased the MDA levels significantly (*, $p < 0.0001$) with respect to the oxidative stress-induced group. Quer: quercetin, QL: quercetin-loaded liposomes, $t$-BHP: *tert*-butyl hydroperoxide, PRBC: packed red blood cells.

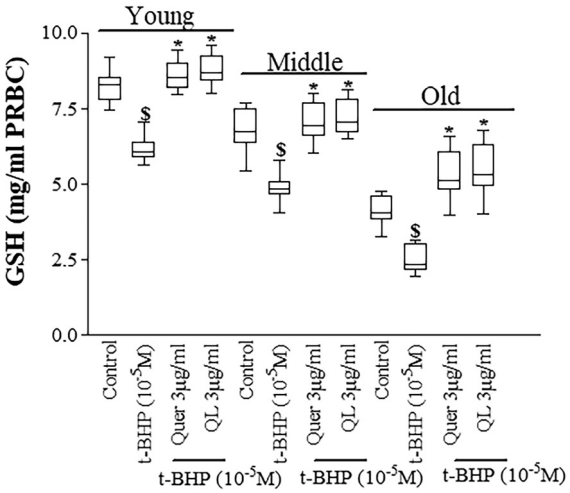


**Fig. 7** The effects of quercetin and quercetin-loaded liposome treatment (3 μg ml$^{-1}$) on GSH content in oxidatively stressed red blood cells of different age groups, *i.e.*, young (20–35 years; $n$ = 11), middle (36–60 years; $n$ = 14), and old (>60 years; $n$ = 6) people. The GSH levels were measured in mg mL$^{-1}$ PRBCs. $t$-BHP ($10^{-5}$ M) was used as an oxidative stress inducer. PRBCs incubated with $t$-BHP exhibited significantly decreased GSH levels ($, $p < 0.0001$) compared to control. The quercetin and quercetin-loaded liposome treatment significantly (*, $p < 0.0001$) increased the GSH levels with respect to the oxidative stress-induced group. Quer: quercetin, QL: quercetin-loaded liposomes, $t$-BHP: *tert*-butyl hydroperoxide, and PRBCs: packed red blood cells.

amount of MDA in the cells. The PRBC membrane exhibits indicators of oxidative stress. Glutathione (GSH) is a non-enzymatic antioxidant found in RBCs. The reduced state of the thiol group in enzymes, hemoglobin, and membrane proteins is maintained by the sulfhydryl (SH) group of cysteine in glutathione (GSH).[30] Our results showed that the level of MDA increased with an increase in age. Our findings were supported by earlier published data that found a direct correlation between age and MDA levels, *i.e.* the MDA level increased with age.[31,32] During the process of aging, the level of the lipid biomarker of oxidative stress, *i.e.*, MDA, is upregulated, while the non-enzymatic antioxidant GSH decreased as also stated by earlier published data.[31–35] The results obtained in this study explained that oxidative stress is a primary contributor to the process of aging and age-related diseases. Quercetin is a flavonoid and plays a role in quenching the reactive oxygen species. We hypothesized that quercetin stops the chain reaction by donating hydrogen and electrons to the free radicals or by upregulating the formation of antioxidants and chelating the metal ions. Quercetin is an effective scavenger of reactive oxygen and nitrogen species like $O2^{\bullet-}$, NO, and ONOO.[36] The existence of two pharmacophores in the quercetin molecule (the OH group at position 3 and the catechol group in the B ring) which has the best configuration for scavenging free rad-

icals has been linked to the compound's antioxidant properties. According to previous literature, quercetin may quench ROS *in vitro*, at concentrations ranging from 5 to 50 μM.[37,38] Since oxidative stress, aging, and a number of diseases are closely related, quercetin-loaded liposome-mediated control of MDA and GSH levels presents promising opportunities. A prominent advantage of our method is its direct applicability to circulating cells like RBCs, which are uniquely sensitive to oxidative damage and relevant to aging. Additionally, the liposomal encapsulation method used here involves passive loading *via* thin-film hydration, which is reproducible and scalable and preserves the antioxidant activity of quercetin. Compared to methods using nanoparticles, micelles, or polymer carriers, liposomes offer higher biocompatibility and hemocompatibility, especially crucial for blood-contact applications.[39] In our study, the drop in MDA levels points to a potential slowdown of aging-related cellular damage, while the rise in GSH levels indicates a more robust cellular defense against oxidative stress as shown in Fig. 6 and 7. Our results emphasize that quercetin also quenches ROS at 3 μg $ml^{-1}$ concentration in RBCs.

## Conclusions

The current study revealed that quercetin and its liposomal formulation decrease the oxidative stress induced by *t*-BHP in red blood cells. One potential solution to quercetin's bioavailability limitations and to fully utilize its potential to slow down the aging process is through the use of quercetin-loaded liposomes. It was found that treatment with quercetin and quercetin-loaded liposomes decreased the MDA content and increased the GSH level in oxidatively stressed red blood cells. Quercetin-loaded liposomes have a higher antioxidant effect than free quercetin so quercetin-loaded liposomes may be used to delay the aging process. This novel approach has important ramifications for developing successful anti-aging therapies that use quercetin as the main therapeutic agent. Even though our *in vitro* results are encouraging, more investigation is necessary to confirm and convert these results into useful treatment plans.

## Data availability

The datasets supporting the findings of this study are available from the corresponding author upon reasonable request. The raw and processed data generated during the current study can be accessed through the provided link https://drive.google.com/drive/folders/13PNjtpYPOU9FsKw6RQCZ-3UO-fOdkClV?usp=drive_link.

## Conflicts of interest

There are no conflicts to declare.

## Acknowledgements

This study was supported by a fellowship (Senior Research Fellow) from the Council of Scientific and Industrial Research (CSIR), Government of India, to Mr Akshay Kumar (09/1152 (0016)/2019-EMR-I). Stuti Bhagat thanks the Indian Council of Medical Research for providing a senior research fellowship. Kareena Moar is a recipient of a junior research fellowship from the Haryana State Council for Science, Innovation and Technology (HSCIT-3946).

## References

1 L. Gil, W. Siems, B. Mazurek, J. Gross, P. Schroeder, P. Voss and T. Grune, *Free Radical Res.*, 2006, **40**, 495–505.
2 G. E. Kisby, S. G. Kohama, A. Olivas, M. Churchwell, D. Doerge, E. Spangler, R. de Cabo, D. K. Ingram, B. Imhof, G. Bao and Y. W. Kow, *Exp. Gerontol.*, 2010, **45**, 208–216.
3 P. Sen, P. P. Shah, R. Nativio and S. L. Berger, *Cell*, 2016, **166**, 822–839.
4 E. Maldonado, S. Morales-Pison, F. Urbina and A. Solari, *Antioxidants*, 2023, **12**, 651.
5 R. Franco, O. J. Schoneveld, A. Pappa and M. I. Panayiotidis, *Arch. Physiol. Biochem.*, 2007, **113**, 234–258.
6 J. B. Owen and D. A. Butterfield, *Methods Mol. Biol.*, 2010, **648**, 269–277.
7 D. Tsikas, S. A. Tsikas, M. Mikuteit and S. J. B. Ückert, *Biomedicines*, 2023, **11**, 2744.
8 P. K. Maurya, P. Kumar and P. Chandra, *World J. Methodol.*, 2015, **5**, 216–222.
9 A. V. Anand David, R. Arulmoli and S. Parasuraman, *Pharmacogn. Rev.*, 2016, **10**, 84–89.
10 N. Lotfi, Z. Yousefi, M. Golabi, P. Khalilian, B. Ghezelbash, M. Montazeri, M. H. Shams, P. Z. Baghbadorani and N. Eskandari, *Front. Immunol.*, 2023, **14**, 1077531.
11 I. U. H. Bhat and R. Bhat, *Biology*, 2021, **10**, 586.
12 X. Yang, D. Wu, Z. Du, R. Li, X. Chen and X. Li, *J. Agric. Food Chem.*, 2009, **57**, 3431–3435.
13 Z. Cui, X. Zhao, F. K. Amevor, X. Du, Y. Wang, D. Li, G. Shu, Y. Tian and X. Zhao, *Front. Immunol.*, 2022, **13**, 943321.
14 A. Kumar and P. K. Maurya, *J. Membr. Biol.*, 2021, **254**, 459–462.
15 P. B. S. de Albuquerque, M. P. de Souza, A. I. Bourbon, M. A. Cerqueira, L. Pastrana, P. Jauregi, J. A. Teixeira and M. J. A. N. das Graças Carneiro-da-Cunha, *Applied Nano*, 2023, **4**, 159–177.
16 H. Nsairat, D. Khater, U. Sayed, F. Odeh, A. Al Bawab and W. Alshaer, *Heliyon*, 2022, **8**, e09394.
17 T. Chen, T. Gong, T. Zhao, Y. Fu, Z. Zhang and T. Gong, *Eur. J. Pharm. Sci.*, 2018, **111**, 293–302.
18 S. Melchior, M. Codrich, A. Gorassini, D. Mehn, J. Ponti, G. Verardo, G. Tell, L. Calzolai and S. J. F. C. Calligaris, *Food Chem.*, 2023, **428**, 136680.
19 M. A. Abdelbari and S. Mosallam, *J. Liposome Res.*, 2025, 1–9.

20 L. Tang, K. Li, Y. Zhang, H. Li, A. Li, Y. Xu and B. Wei, *Sci. Rep.*, 2020, **10**, 2440.
21 M. T. Luiz, J. A. P. Dutra, L. B. Tofani, J. T. C. de Araújo, L. D. Di Filippo, J. M. Marchetti and M. Chorilli, *Pharmaceutics*, 2022, **14**, 821.
22 V. De Leo, A. M. Maurelli, L. Giotta and L. Catucci, *Colloids Surf., B*, 2022, **218**, 112737.
23 C. Bonechi, A. Donati, G. Tamasi, G. Leone, M. Consumi, C. Rossi, S. Lamponi and A. Magnani, *Biophys. Chem.*, 2018, **233**, 55–63.
24 S. Singh, R. Asal and S. Bhagat, *J. Biomed. Mater. Res., Part A*, 2018, **106**, 3152–3164.
25 P. K. Maurya and S. I. Rizvi, *Nat. Prod. Res.*, 2009, **23**, 1072–1079.
26 E. Beutler, O. Duron and B. M. Kelly, *J. Lab. Clin. Med.*, 1963, **61**, 882–888.
27 M. Buchweitz, P. A. Kroon, G. T. Rich and P. J. Wilde, *Food Chem.*, 2016, **211**, 356–364.
28 D. Liu, H. Hu, Z. Lin, D. Chen, Y. Zhu, S. Hou and X. Shi, *J. Photochem. Photobiol., B*, 2013, **127**, 8–17.
29 C. Uchendu, S. F. Ambali, J. O. Ayo, K. A. N. Esievo and A. J. Umosen, *Toxicol. Rep.*, 2014, **1**, 373–378.
30 A. Mariano, I. Bigioni, F. Misiti, L. Fattorini, A. Scotto d'Abusco and A. Rodio, *Curr. Issues Mol. Biol.*, 2022, **44**, 3481–3495.
31 P. K. Maurya, P. Kumar, S. Nagotu, S. Chand and P. Chandra, *RSC Adv.*, 2016, **6**, 53195–53202.
32 U. Mutlu-Turkoglu, E. Ilhan, S. Oztezcan, A. Kuru, G. Aykac-Toker and M. Uysal, *Clin. Biochem.*, 2003, **36**, 397–400.
33 P. K. Maurya and S. I. Rizvi, *Indian J. Clin. Biochem.*, 2010, **25**, 398–400.
34 M. Erden-Inal, E. Sunal and G. Kanbak, *Cell Biochem. Funct.*, 2002, **20**, 61–66.
35 A. Kumar, S. Bhagat, K. Moar, S. Singh, T. C. Dakal and P. K. Maurya, *BioNanoScience*, 2025, **15**, 1–10.
36 A. W. Boots, G. R. Haenen and A. Bast, *Eur. J. Pharmacol.*, 2008, **585**, 325–337.
37 L. G. Costa, J. M. Garrick, P. J. Roque and C. Pellacani, *Oxid. Med. Cell. Longevity*, 2016, **2016**, 2986796.
38 A. Kaushik, K. Chauhan and S. Singh, in *Treatments, Nutraceuticals, Supplements, and Herbal Medicine in Neurological Disorders*, ed. C. R. Martin, V. B. Patel and V. R. Preedy, Academic Press, 2023, pp. 623–637, DOI: 10.1016/B978-0-323-90052-2.00029-9.
39 T. R. Kyriakides, A. Raj, T. H. Tseng, H. Xiao, R. Nguyen, F. S. Mohammed, S. Halder, M. Xu, M. J. Wu, S. Bao and W. C. Sheu, *Biomed. Mater.*, 2021, **16**, 33578402.